J Physiol 587.23 (2009) pp 5613–5631

The Journal of Physiology

Photostimulation of channelrhodopsin-2 expressing ventrolateral medullary neurons increases sympathetic nerve activity and blood pressure in rats

Stephen B. G. Abbott[1,2], Ruth L. Stornetta[1], Carmela S. Socolovsky[1], Gavin H. West[1] and Patrice G. Guyenet[1]

[1] *Department of Pharmacology, University of Virginia, Charlottesville, VA 22908, USA*
[2] *Australian School of Advanced Medicine, Macquarie University, Sydney, Australia*

To explore the specific contribution of the C1 neurons to blood pressure (BP) control, we used an optogenetic approach to activate these cells *in vivo*. A lentivirus that expresses channelrhodopsin-2 (ChR2) under the control of the catecholaminergic neuron-preferring promoter PRSx8 was introduced into the rostral ventrolateral medulla (RVLM). After 2–3 weeks, ChR2 was largely confined to Phox2b-expressing neurons (89%). The ChR2-expressing neurons were non-GABAergic, non-glycinergic and predominantly catecholaminergic (∼54%). Photostimulation of ChR2-transfected RVLM neurons (473 nm, 20 Hz, 10 ms, ∼9 mW) increased BP (15 mmHg) and sympathetic nerve discharge (SND; 64%). Light pulses at 0.2–0.5 Hz evoked a large sympathetic nerve response (16 × baseline) followed by a silent period (1–2 s) during which another stimulus evoked a reduced response. Photostimulation activated most (75%) RVLM baroinhibited neurons sampled with 1/1 action potential entrainment to the light pulses and without accommodation during 20 Hz trains. RVLM neurons unaffected by either CO_2 or BP were light-insensitive. Bötzinger respiratory neurons were activated but their action potentials were not synchronized to the light pulses. Juxtacellular labelling of recorded neurons revealed that, of these three cell types, only the cardiovascular neurons expressed the transgene. In conclusion, ChR2 expression had no discernable effect on the putative vasomotor neurons at rest and was high enough to allow precise temporal control of their action potentials with light pulses. Photostimulation of RVLM neurons caused a sizable sympathoactivation and rise in blood pressure. These results provide the most direct evidence yet that the C1 neurons have a sympathoexcitatory function.

(Received 26 June 2009; accepted after revision 7 October; first published online 12 October 2009)
Corresponding author P. G. Guyenet: University of Virginia Health System, PO Box 800735, 1300 Jefferson Park Avenue, Charlottesville, VA 22908-0735, USA. Email: pgg@virginia.edu

Abbreviations C1 neurons, subset of lower brainstem adrenergic neurons; ChR2, channelrhodopsin-2; Phox2b, paired-like homeobox 2b; PND, phrenic nerve discharge; RTN, retrotrapezoid nucleus; RVLM, rostral ventrolateral medulla; SND, sympathetic nerve discharge; TH, tyrosine hydroxylase; VGLUT2, vesicular glutamate transporter 2

Introduction

The rostral ventrolateral medulla (RVLM) is an important nodal point for BP control and sympathetic vasomotor tone generation (Guertzenstein & Silver, 1974; Dampney *et al.* 1982; Ross *et al.* 1984; Pilowsky & Goodchild, 2002; Guyenet, 2006). The pivotal neurons are presumed to be cells that are strongly inhibited by activation of arterial baroreceptors (barosensitive or 'cardiovascular' neurons) and directly innervate the sympathetic preganglionic neurons (Barman & Gebber, 1985; Brown & Guyenet, 1985; Guyenet, 2006). This cell population includes the C1 neurons, which have a mixed adrenergic/glutamatergic phenotype, and non-catecholaminergic neurons, which are also presumably glutamatergic (Milner *et al.* 1988; Lipski *et al.* 1995; Jansen *et al.* 1995*a*; Schreihofer & Guyenet, 1997; Stornetta *et al.* 2002*a*; Card *et al.* 2006).

Chemical or electrical stimulation of the RVLM increases arterial pressure by as much as 70 mmHg in anaesthetized rodents (Goodchild *et al.* 1984; Ross *et al.* 1984; Brown & Guyenet, 1985). This effect is due to a rise in sympathetic tone and, since the 1980s, it has been largely attributed to the activation of the C1 cells and, even more restrictively, to the monosynaptic

DOI: 10.1113/jphysiol.2009.177535

connection that exists between these neurons and sympathetic preganglionic neurons (Reis *et al.* 1988). However, this plausible interpretation still rests on physiological evidence that is far from compelling. Although the C1 cells represent the bulk of the RVLM neurons that innervate the sympathetic preganglionic neurons (∼70%), the proportion of these C1 cells that regulate the cardiovascular system as opposed to other sympathetically innervated tissues is uncertain (Jansen *et al.* 1995*a*). In addition, the C1 cells have innumerable targets besides the preganglionic neurons (Card *et al.* 2006). These projections could be activating a distributed sympathetic tone generating network ('oscillator') of the type proposed by Barman and Gebber (e.g. Gebber *et al.* 1995) and could conceivably be equally or more important for BP control than those that are directed to the spinal cord. Also, massive lesions of the C1 catecholaminergic cells, while attenuating the sympathoexcitatory responses mediated by RVLM stimulation, do not perceptibly alter resting sympathetic tone in anaesthetized rats and reduce resting mean arterial pressure by a mere 10 mmHg in the unanaesthetised state (Schreihofer *et al.* 2000; Madden & Sved, 2003). Finally, as few as 1–2% of the synapses located within the intermediolateral cell column may originate from the C1 cells which, if correct, suggests that the preganglionic neurons must be primarily regulated by other cells (Llewellyn-Smith *et al.* 1991). Together, these facts paint a less clear-cut picture of the role of the C1 neurons in cardiovascular regulation than generally assumed. Much of this uncertainty comes from the fact that it has not been possible so far to selectively activate the C1 neurons *in vivo*.

To gain further insight into the role of the C1 neurons, we used the optogenetic channelrhodopsin-2 (ChR2) approach developed by Deisseroth and colleagues to control the activity of the C1 neurons with light pulses *in vivo* (Nagel *et al.* 2003; Boyden *et al.* 2005; Adamantidis *et al.* 2007). An enhanced form of ChR2 (H134R mutation) was introduced into the C1 neurons using a lentivirus that expresses this protein under the control of the catecholaminergic neuron-selective artificial promoter PRSx8 (Hwang *et al.* 2001; Duale *et al.* 2007). A fusion protein between ChR2 and the fluorescent protein mCherry provided histological identification of the ChR2-expressing cell bodies and their axonal projections (Adamantidis *et al.* 2007).

In this study we demonstrate that the activity of the ChR2-transfected C1 cells can be efficiently controlled by photostimulation. We also show that relatively selective stimulation of the C1 cells reproduces many of the cardiovascular effects elicited by conventional (electrical or chemical) stimulation of the RVLM providing more direct evidence that the activation of the C1 cells does have a powerful stimulatory effect on sympathetic vasoconstrictor tone.

Methods

Animal use was in accordance with guidelines approved by the University of Virginia Animal Care and Use Committee (ACUC). The University of Virginia ACUC uses criteria in conformity with the ethical standards described by Drummond (2009). Experiments were conducted on 22 adult male Sprague–Dawley rats (weight ranging from 280 to 410 g).

Plasmid and virus preparation

The lentiviral vector was prepared using a previously described construct (pLenti-PRSx8-hChR2(H134R)-mCherry-WPRE; abbreviated PRSx8-ChR2-mCherry) which features the Phox2-binding artificial promoter PRSx8 and an enhanced version of the photoactivatable cationic channel ChR2 (H134R) fused to the fluorescent protein mCherry (Abbott *et al.* 2009). The virus was produced using a slight modification of our previous protocol. Specifically, psPAX2 (Addgene plasmid 12260) was used as the packaging plasmid rather than pCMVdeltaR8.74.

We assessed virus titre by DNA analysis of transduced HEK293 cells because this method provides a reliable estimate of functional titres and can be applied regardless of the specific transgene (Sastry *et al.* 2002). Approximately 30 000 HEK293 cells (ATCC, Manassas, VA, USA) were plated per well on a 24-well plate and two wells each were infected overnight with 1 μl, 0.1 μl or 0.01 μl of lentivirus in 350 μl DMEM/F12 growth medium. After 4 days, the cells were harvested; genomic DNA was extracted and purified (PureLink Genomic DNA Mini Kit, Invitrogen, Carlsbad, CA, USA). Two dilutions of the DNA from each sample of the virus-infected cells were subjected to quantitative PCR with the MyiQ Single Color Real-Time PCR Detection System (Bio-Rad, Hercules, CA, USA) using primers appropriate for the detection of the DNA sequence encoding mCherry (5′-AGA TCA AGC AGA GGC TGA AGC TGA-3′ forward and 5′-TGT GGG AGG TGA TGT CCA ACT TGA-3′ reverse). Titre determination was therefore based on 24 qPCR measurements (three initial viral dilutions in duplicate wells and two dilutions of the DNA extracted from each well run in duplicate). The PCR programme was an initial cycle of 3 min at 95°C, followed by 40 cycles of 95°C for 15 s, 58°C for 40 s and 72°C for 40 s followed by 1 cycle of 72°C for 1 min. After another denaturation step at 95°C for 1 min, a melt curve was generated with 0.5°C steps every 10 s starting at 60°C and ending at 100°C. Sufficient amounts of DNA were used to obtain a detection threshold in the linear range (15–28 amplification cycles). Integrity of genomic DNA was verified by qPCR amplification of hGAPDH with the same concentrations of genomic DNA (data not shown). Known amounts of the PRSx8-ChR2-mCherry

DNA plasmid, determined by spectrophotometry, were used to generate a standard curve. The standard curve was then used to calculate the number of copies of transgene DNA incorporated into the host cells' DNA. The final titre was therefore expressed as the number of molecules of transgene DNA incorporated per well of HEK cells and normalised per ml of virus. The batch of virus used in the present experiments registered at 1.8×10^{10} transgene DNA molecules incorporated per ml.

Injections of lentivirus into the rostral ventrolateral medulla

The PRSx8-hChR2 (H134R)-mCherry virus was injected into the RVLM in rats (Sprague–Dawley, males, weight: 210–250 g) that were anaesthetized with a mixture of ketamine (75 mg kg^{-1}), xylazine (5 mg kg^{-1}) and acepromazine (1 mg kg^{-1}) administered I.M. Anaesthetised animals had no response to skin incision or strong toe pinch. Surgery used standard aseptic methods. The rats received injections of the antibiotic ampicillin (100 mg kg^{-1}, I.M.) and the analgesic ketorolac (0.6 mg kg^{-1}, I.P.) after surgery. These drugs were re-administered 20 h later. The lentivirus was delivered by pressure through glass pipettes as previously described (Abbott *et al.* 2009). Injections (200 nl per site over 5 min) were made unilaterally at two sites within the left RVLM. The rostral injection was made at the caudal edge of the facial motor nucleus, 1.8 mm lateral to the midline and at a depth corresponding to the bottom of the nucleus (8.5–9.1 mm below the cerebellar surface). The caudal and inferior limits of the facial motor nucleus were determined by recording antidromic field potentials through the pipette that contained the virus as described previously (Abbott *et al.* 2009). The second injection was made 400 μm caudal to the first and at the same depth and lateral coordinate. Animals were maintained for 10–21 days before they were used in physiological experiments. The surgical procedures and virus injections produced no observable behavioural or respiratory effects and these rats gained weight normally.

Physiological preparation

Surgical anaesthesia was induced with 5% isoflurane in 100% oxygen and maintained via a tracheostomy by ventilating the rats with 3.0–3.5% isoflurane in 100% oxygen. The following previously described surgical procedures were used in all rats: insertion of a venous femoral line and an arterial line (common carotid or femoral), exposure of the left mandibular branch of the facial nerve for antidromic mapping of the facial motor nucleus, and dissection of the splanchnic nerve distal to the aorticorenal ganglion (Guyenet *et al.* 2005; Moreira *et al.* 2006). The following three additional procedures were performed only in the rats that were used for unit recording: subdiaphragmatic placement of an aortic cuff to manipulate BP by restricting blood flow, dissection of the phrenic nerve in the neck and laminectomy at thoracic level T3 for insertion of a bipolar stimulating electrode. The intact splanchnic nerve and the cut phrenic nerve were mounted on bipolar electrodes and buried in biocompatible polymer (World Precision Instruments, Sarasota, FL, USA) for multi-fibre recording. Rats were placed prone in a Kopf stereotaxic frame with the bite bar set at negative 3.5 mm. A small portion of the occipital plate was removed to allow trans-cerebellar access to the RVLM. Phenylephrine (PE; 10 μg kg^{-1}) was injected I.V. to raise arterial pressure in rats in which an aortic cuff had not been placed. Sodium nitroprusside (SNP; 10 μg kg^{-1}) was used to lower BP in selected rats. In rats used for unit recording, a bipolar stimulating electrode was inserted 0.8 mm lateral of midline and 1.0 mm ventral to the dorsal surface into the spinal cord (T3) in order to test whether subsets of RVLM neurons had spinal axons (0.5 ms current pulses, 0.1–2 mA) (Brown & Guyenet, 1985). Rectal temperature was maintained at 37.5 $\pm$ 0.5°C. End-tidal CO_2 (P_{ETCO_2}), continuously monitored with a micro-capnometer (Columbus Instruments, Columbus, OH, USA), was maintained between 3.5 and 4.5% at rest and modified as needed by changing the ventilation parameters or adding CO_2 to the oxygen.

Upon completion of surgical procedures, isoflurane was gradually withdrawn while freshly prepared α-chloralose was infused (Fisher Scientific, Fair Lawn, NJ, USA; dissolved in 2% sodium borate; initial dose 70 mg kg^{-1}; additional doses of 20 mg kg^{-1} as required, see below) and ventilation with 100% O_2 was continued. Chloralose was used because all other anaesthetics that we have examined (halothane, isoflurane, urethane I.P. or I.V.) cause the blood pressure regulating neurons of the RVLM to discharge at a very high rate at rest (up to 35 Hz), a particularly unfavourable baseline condition to examine the effect caused by their activation. Following the initial administration of α-chloralose, rats were allowed to stabilize for 30 min. During this initial period the adequacy of the anaesthesia was assessed by the absence of withdrawal reflex and BP changes to a firm paw pinch. The muscle relaxant pancuronium was administered prior to the recordings (initial dose 1 mg kg^{-1} I.V. plus additional 0.2 mg kg^{-1} doses if needed). Thereafter the adequacy of the anaesthesia was judged by the fact that BP increased less than 10 mmHg in response to firm toe or tail pinch and, when the phrenic nerve was recorded, failed to raise the activity of this nerve. Three to five supplemental doses of chloralose (20 mg kg^{-1} each) were administered, typically every 45 min, during a recording experiment lasting up to 3 h.

Photostimulation of the ventrolateral medulla

The light source was a diode pumped 473 nm blue laser (CrystaLaser Model BC-473-060-M; Reno, NV, USA) controlled by a function generator (Grass Technologies/Astro-Med Inc., Warwick, RI, USA) to generate 10 ms light pulses. Except for experiments involving unit recordings, a 200 μm diameter fibre optic (Thorlabs, Newton, NJ, USA) was inserted vertically through the cerebellum as previously described (Abbott *et al.* 2009). The optimal placement was determined in each rat by mapping the contour of the facial motor nucleus with antidromic field potentials using a glass pipette before inserting the fibre optic. Based on the updated coordinates of the facial motor nucleus, the optical fibre was placed 300–500 μm dorsal to the ventral extent and 200–300 μm caudal of the caudal pole to the facial nucleus where most ChR2-expressing neurons were located. In experiments that required recording of RVLM units, the fibre optic was inserted at a 20 deg angle in the transverse plane from the contralateral side. Stimulation trials generally consisted of 10–30 s trains of 10 ms pulses delivered at 20 Hz. In some experiments, single or paired 10 ms pulses were generated at low frequency (0.3–0.5 Hz). The output of the laser was set at a nominal 12 mW determined when the laser was activated in continuous mode. The actual power output measured at the end of the fibre optic with a light meter (Thorlabs, Newton, NJ, USA), was close to 9 mW. The same fibre optic was used for all experiments and the power output was chosen empirically based on our previous study (Abbott *et al.* 2009), the selection criteria being efficacy, reproducibility of the effects over a 3 h period and lack of tissue lesion in the histological material other than the slight mechanical damage expected from the insertion of a 200 μm-thick object. The power setting of the laser was kept constant for all the experiments and does not necessarily represent the optimal light intensity.

Single unit recordings of RVLM neurons

Single-unit recordings were made with glass pipettes filled with 2 M NaCl (8–14 MΩ) and, in experiments designed to label the recorded neurons, the pipettes contained 5% (w/v) biotinamide in 0.5 M sodium acetate (18–22 MΩ). The caudal and lower boundaries of the facial motor nucleus were determined by a preliminary mapping of antidromic field potentials evoked by stimulating the facial branch of the facial nerve. Unit recordings were then obtained 0–500 μm caudal to the facial motor nucleus, 1.5–2.1 mm lateral to the midline and from 0 to 500 μm dorsal to a depth corresponding to the lower edge of the facial motor nucleus. The sampled region encompasses the RVLM and the overlying Bötzinger region.

We only recorded from RVLM neurons that were active at rest. These neurons were classified into four categories: cardiovascular, tonic, respiratory and retrotrapezoid-like (RTN-like). Cardiovascular neurons were strongly inhibited by acute increases in BP and relatively insensitive to changes in P_{CO_2}, and had relatively little respiratory modulated activity. In some experiments, these cells were shown to have axonal projections to the spinal cord (T3) using antidromic activation and the collision test. Tonic cells had a regular discharge that was insensitive to changes in BP and CO_2. Respiratory neurons were defined as neurons with ON–OFF discharges synchronized with respiration. They were sub-classified according to the relationship between their burst and the phrenic nerve discharge. RTN-like neurons were moderately active at rest (4–10 Hz), silenced by lowering end-tidal CO_2 below 3–4% and virtually insensitive to BP elevation (Guyenet *et al.* 2005). Photostimulation of cells displaying characteristics consistent with RTN neurons have been previously investigated (Abbott *et al.* 2009) and these cells were excluded from the present report.

Data acquisition and processing, statistics

All analog data were acquired on a computer via a micro1401 digitizer (Cambridge Electronic Design (CED), Cambridge, UK) and were processed off-line using Spike 5 software (CED) as described (Guyenet *et al.* 2005). Integrated splanchnic nerve discharge (isSND) was obtained after rectification and smoothing ($\tau = 2$ s) of the original signal, which was acquired with a 100–3000 Hz band pass. Except where indicated, iSND was normalized within animals by assigning a value of 100 to resting SND and a value of 0 to the minimum value recorded at saturation of the baroreflex during either administration of PE (10 μg kg^{-1}; I.V.) or gradual aortic occlusion.

The relationship between resting MAP and sSND was investigated by first normalizing SND between saturation (0%) during gradual aortic occlusion and maximum SND produced by I.V. infusion of SNP (100%). Photostimulation trials during aortic occlusion or SNP infusion produced *X*–*Y* data points that were placed into three groups according to arterial pressure. The differences between resting and photostimulation evoked SND across these groups were compared using a regular one-way ANOVA with multiple *t* tests and Bonferroni's correction.

Statistical analysis was done using GraphPad 10 software. Student's unpaired *t* test and one- and two-way ANOVA were used as appropriate. All grouped values are presented as means ± S.E.M., except where noted.

Differences where $P < 0.05$ were considered statistically significant.

Histology

At the end of the physiological procedures the rats were deeply anaesthetized by re-administering 5% isoflurane until their BP was reduced to 30 mmHg. They were immediately perfused with a heparin solution followed by a saline rinse and buffered 4% paraformaldehyde. After 1–2 days of post-fixation, 30 μm-thick coronal sections were cut with a vibrating microtome according to previously established procedures (Kang *et al.* 2007). The transcription factor Phox2b, tyrosine hydroxylase (TH) and mCherry were detected by immunohistochemistry using antibodies against Phox2b (rabbit anti-Phox2b was a gift from J.-F. Brunet, Ecole Normale Supérieure, Paris, France), TH (mouse monoclonal anti-TH; Chemicon, Temecula, CA, USA) and dsRed (recognizes mCherry; rabbit anti-dsRed, Clontech, Mountain View, CA, USA). Antibodies were visualized with the fluorescent secondary antibodies donkey anti-rabbit Cy3 (Jackson Immuno-Research Laboratories, West Grove, PA, USA) or donkey anti-mouse Alexa488 (Molecular Probes, Eugene, OR, USA). The antibodies used and their specificity have been described previously (Kang *et al.* 2007; Abbott *et al.* 2009).

Histological detection of pre-pro-galanin mRNA, pre-pro-NPY mRNA and GAD67 mRNA by non-radioactive *in situ* hybrization histochemistry (ISH) was performed exactly as previously described (Stornetta & Guyenet, 1999; Stornetta *et al.* 1999; Stornetta *et al.* 2009). Pre-pro-galanin is a specific marker for 50% of the RTN neurons (Stornetta *et al.* 2009), pre-pro-NPY is selectively expressed by a large subset of C1 neurons (Stornetta *et al.* 1999). GAD67, a specific marker of GABAergic neurons, is expressed neither by RTN neurons nor by the C1 cells (Stornetta & Guyenet, 1999; Stornetta *et al.* 2006). ISH was combined with the immunofluorescent detection of mCherry using rabbit anti-dsRed (Clontech) to identify the mRNA content of the ChR2-expressing neurons.

Mapping and cell counting

All histological material was examined and photographed using a Zeiss Axioimager Z1 (Carl Zeiss Microimaging, Thornwood, NY, USA) with a Zeiss Axiocam MRc digital camera (basic resolution 1388 × 1040 pixels). For estimation of the number and phenotype of transfected neurons, a one in six series of 30 μm coronal sections that encompassed the transfected brain area (from 7–10 sections/rat) was plotted using the Neurolucida computer assisted graphing software as previously described (Stornetta *et al.* 2002*a*).

Results

PRSx8-ChR2-mCherry expression is selective for Phox2b neurons in the RVLM

Injections of the lentivirus PRSx8-ChR2-mCherry into the left RVLM produced intense mCherry expression only in neurons. Consistent with our previous study (Abbott *et al.* 2009) most of the mCherry-positive neurons contained Phox2b (89 ± 1% based on counts from 5 representative cases; not illustrated). Figure 1*A* shows the anatomical distribution of the mCherry-positive cells in a representative case. These neurons were always located in close proximity to the original injection site and were concentrated in the region of the ventrolateral reticular formation that lies below the caudal end of the facial motor nucleus and extends up to 500 μm posterior to this level (11.4–12.1 mm caudal to Bregma; Fig. 1*A* and *B*). This region contains the bulk of the C1 and other blood-pressure regulating presympathetic neurons (Schreihofer & Guyenet, 2000). Its rostral extent overlaps substantially with the retrotrapezoid nucleus (RTN) (Stornetta *et al.* 2006). Figure 2*B* shows the average rostro-caudal distribution of TH- positive and TH-negative neurons expressing mCherry for 12 rats. On average 54 ± 3% of the mCherry-positive neurons were immunoreactive (ir) for TH out of a total of 153 ± 13 mCherry-positive neurons counted per rat in a 1 in 6 series of 30 μm-thick transverse sections from 12 rats (8–10 sections/rat counted). A rough estimate of the number of ChR2-transfected neurons (918 per rat on average) can be calculated from these counts, 495 of which were C1 neurons. These figures probably overestimate the actual cell numbers by around 20% because they did not rely on unbiased stereological methods for their calculation.

In the RVLM proper (Bregma levels 11.78 or 12.1 mm in Fig. 1*A*), mCherry was detected in neurons that contained VGLUT2 mRNA (Fig. 2*A*) and, occasionally, NPY mRNA (Fig. 2*B*). At more rostral and ventral levels corresponding primarily to the retrotrapezoid nucleus (RTN, e.g. bregma −11.42 mm, Fig. 1*A*), mCherry was detected in very superficial neurons that contained VGLUT2 mRNA (Fig. 2*C*) and pre-pro-galanin mRNA (Fig. 2*D*). mCherry was almost never identified in GAD67 mRNA-containing neurons (Fig. 2*E*). More precisely, only 4 of 177 mCherry positive neurons counted in four representative rats were GAD67 mRNA-positive. No GlyT2 mRNA-positive neurons were found to express mCherry (Fig. 2*F*). Of note, GlyT2 mRNA-positive neurons are absent from the RTN but are plentiful 100 μm or more dorsal to the C1 cells.

Based on cells counts from four rats, 70 ± 2% of the TH-positive neurons located between Bregma levels 11.4

and 12.1 mm and within the RVLM proper (the triangular region bounded by the nucleus ambiguus dorsally, the spinal trigeminal tract and the pyramidal tract laterally, Fig. 1*A*) expressed ChR2-mCherry. This triangle excludes a sizable portion of the C1 cells that have a more medial location (Ruggiero *et al.* 1985). These medial C1 cells were not transfected. When these more medial TH-positive cells were included in the counts, the proportion of C1 cells located between Bregma levels 11.4 and 12.1 mm that expressed ChR2-mCherry was only 54 ± 3%.

This evidence indicates that ChR2 was expressed overwhelmingly by excitatory neurons (neither GABAergic nor glycinergic) that were almost all Phox2b-positive. This population included a slight majority of C1 cells (54%) some of which expressed NPY mRNA. The balance consisted mostly of putative RTN neurons (TH-negative, VGLUT2 mRNA-positive), some of which were definitively identified as such by the presence of the selective marker pre-pro-galanin mRNA (Stornetta *et al.* 2009). A small proportion of the ChR2-transfected TH-negative neurons, particularly those located dorsal to the bulk of the C1 cells, could also have been cholinergic autonomic motor neurons (Abbott *et al.* 2009).

Photostimulation of the RVLM increases arterial pressure and SND

Photostimulation of the left RVLM (30 s; 20 Hz, 10 ms pulses, ~9 mW), the side containing ChR2-expressing neurons, raised SND, AP and the HR (Fig. 3*A*). Typically, AP increased steadily over time and reached a maximum towards the end of the stimulus. The SND response consisted of a large initial burst at the onset of the stimulus period which was followed by a steady-state discharge greater than the resting level. Usually, the steady-state had a slightly decrementing pattern that mirrored the gradual rise in BP, indicative of baroreceptor feedback. At the end of the stimulus, SND decreased abruptly then recovered gradually as BP returned to the pre-stimulus level (Fig. 3*A*). This undershoot was also presumably due to baroreceptor feedback. When examined at a higher time resolution, SND was activated in bursts that were synchronized with each light pulse (Fig. 3*B*). Photostimulation produced a very small tachycardia in the case illustrated in Fig. 3*A*.

These observations were reproducible. On average, RVLM photostimulation on the ChR2-transfected side (20 Hz, 30 s, 10 ms pulses, 7–10 mW) produced significant

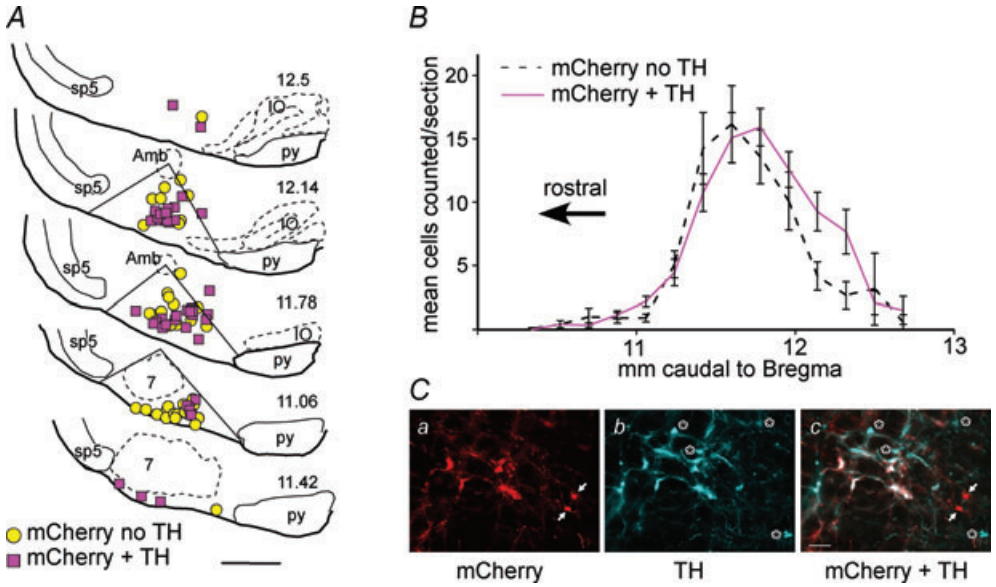

Figure 1. PRSx8-channel rhodopsin2 (ChR2)-mCherry-expressing neurons and their distribution in the ventral medulla

A, computer assisted plots of mCherry-expressing neurons in several coronal planes from a representative case. Circles represent non-tyrosine hydroxylase (TH) immunoreactive (ir) neurons that express the ChR2-mCherry fusion protein. Squares represent mCherry-expressing neurons that are also TH-ir. Numbers on the right hand side of each drawing are the mm caudal to bregma after the atlas of Paxinos & Watson (2005). Scale bar is 500 μm. Abbreviations: 7, facial motor nucleus; Amb, ambiguus nucleus; IO, inferior olivary nucleus; py, pyramidal tract, sp5, spinal trigeminal tract. *B*, average number of counted neurons per section from 12 rats. Counts were made from a 1 in 6 series of 30 μm coronal sections. Error bars represent S.E.M. *C*, digital images of neurons in the C1 area of the ventral lateral medulla from the case illustrated in panel *A* Bregma level 12.14. *a*, neurons expressing ChR2 mCherry revealed with immunofluorescence for DsRed. *b*, C1 neurons revealed with immunofluorescence for TH. *c*, merge of *a* and *b*. Note neurons expressing mCherry only (arrows) or TH only (asterisks). Most of the neurons in this image are double-labelled and appear white. Scale bar is 50 μm.

increases in MAP and SND compared to identical stimulation on the contralateral uninfected side (MAP: $+14.8 \pm 1.6$ *vs.* $+2.2 \pm 1.8$ mmHg; $P < 0.001$, SND: $+63.9 \pm 5.8$ *vs.* $+0.6 \pm 2.6\%$ of baseline; $P < 0.001$, Fig. 3*C*). HR responses were small and variable (range: -3.4 to $+8.5$ bpm). Tachycardia predominated ($n = 9$ of 10) and was presumably a sympathetic response given the strong vagolytic effect of pancuronium used as a muscle relaxant but the HR response failed to reach significance at the group level ($+4.7 \pm 1.3$ *vs.* $+1.4 \pm 1.0$ bpm, $P = 0.15$) (Fig. 3*C*).

The rise in AP and SND produced by photostimulation was inversely correlated with the resting level of BP (Spearman r^2: MAP $= -0.57$, $P < 0.001$, SND $= -0.34$, $P < 0.05$; $n = 10$ rats; Fig. 3*D* and *E*). This relationship was reminiscent of that between resting SND and BP at steady-state; the largest rise in BP and SND was evoked by photostimulation when resting BP was below 90 mmHg and progressively smaller increases were observed in animals with resting BP above that level.

The relationship between the increase in SND caused by photostimulation of the RVLM and the resting BP was more systematically investigated in five rats by repeating the stimulus (20 Hz, 10 ms, 10–20 s, 9 mW) within the same animal while the BP was set at different levels (Fig. 3*F*). The BP was either raised to various extents by restricting blood flow through the descending aorta or lowered below baseline by intravenous injection of nitroprusside. This protocol revealed that, within a given rat, the steady-state increase in SND elicited by RVLM photostimulation was greatest when the baroreflex was unloaded and became progressively smaller as the baroreflex reached saturation ($F_{2,11} = 4.9$; $P = 0.03$) (Fig. 3*Fc*, *G* and *H*).

Photostimulation activates RVLM cardiovascular neurons

Single RVLM neurons were recorded between 0 and 500 μm caudal to the facial motor nucleus, the region that contained the majority of the ChR2-transfected neurons. We examined the effects of repeated exposure of the cells to laser light delivered with a fibre optic inserted at 20 deg

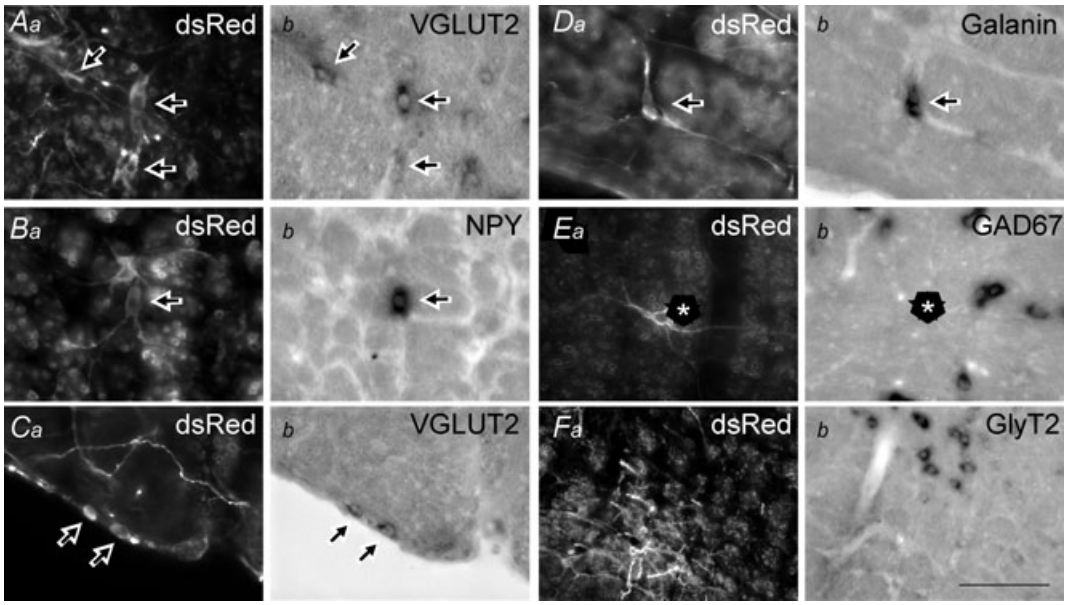

Figure 2. Selective expression of ChR2 by excitatory neurons including subsets of C1 and RTN cells
A, co-localization of the ChR2-mCherry fusion protein and VGLUT2 mRNA in the C1 region of the rostral ventrolateral medulla. mCherry was revealed by immunofluorescence (*Aa*, dsRed, reporter Cy3) and VGLUT2 mRNA by non-radioactive ISH (*Ab*, brightfield). Dual-labelled neurons are indicated by the arrows. *B*, co-localization of the ChR2-mCherry fusion protein (*Ba*, immunofluorescence) and pre-pro-NPY mRNA (*Bb*, ISH, brightfield). In the ventrolateral medulla ppNPY mRNA is a specific marker of a subset of C1 neurons. *C*, co-localization of the ChR2-mCherry fusion protein (*Ca*; immunofluorescence) and VGLUT2 mRNA (*Cb*; ISH, brightfield). These very superficial glutamatergic neurons are a subset of RTN neurons. *D*, co-localization of the ChR2-mCherry fusion protein (*Da*; immunofluorescence) and pre-pro-galanin mRNA (*Db*; ISH, brightfield). ppGal mRNA is a specific marker of a subset of RTN neurons. *E*, the ChR2-mCherry fusion protein (*Ea*; immunofluorescence) and GAD67 mRNA (*Eb*; ISH, brightfield) were not co-localized. Star indicates ChR2-expressing neuron in *Ea* and its location in the brightfield photograph (*Eb*) *F*, the neurons that expressed the ChR2-mCherry fusion protein (*Fa*; immunofluorescence) were always located below the glycinergic cells (*Fb*, GlyT2 mRNA ISH, brightfield). Scale bar shown in *Fb* represents 75 μm for panels *Aa–Eb* and 150 μm for panels *Fa* and *Fb*.

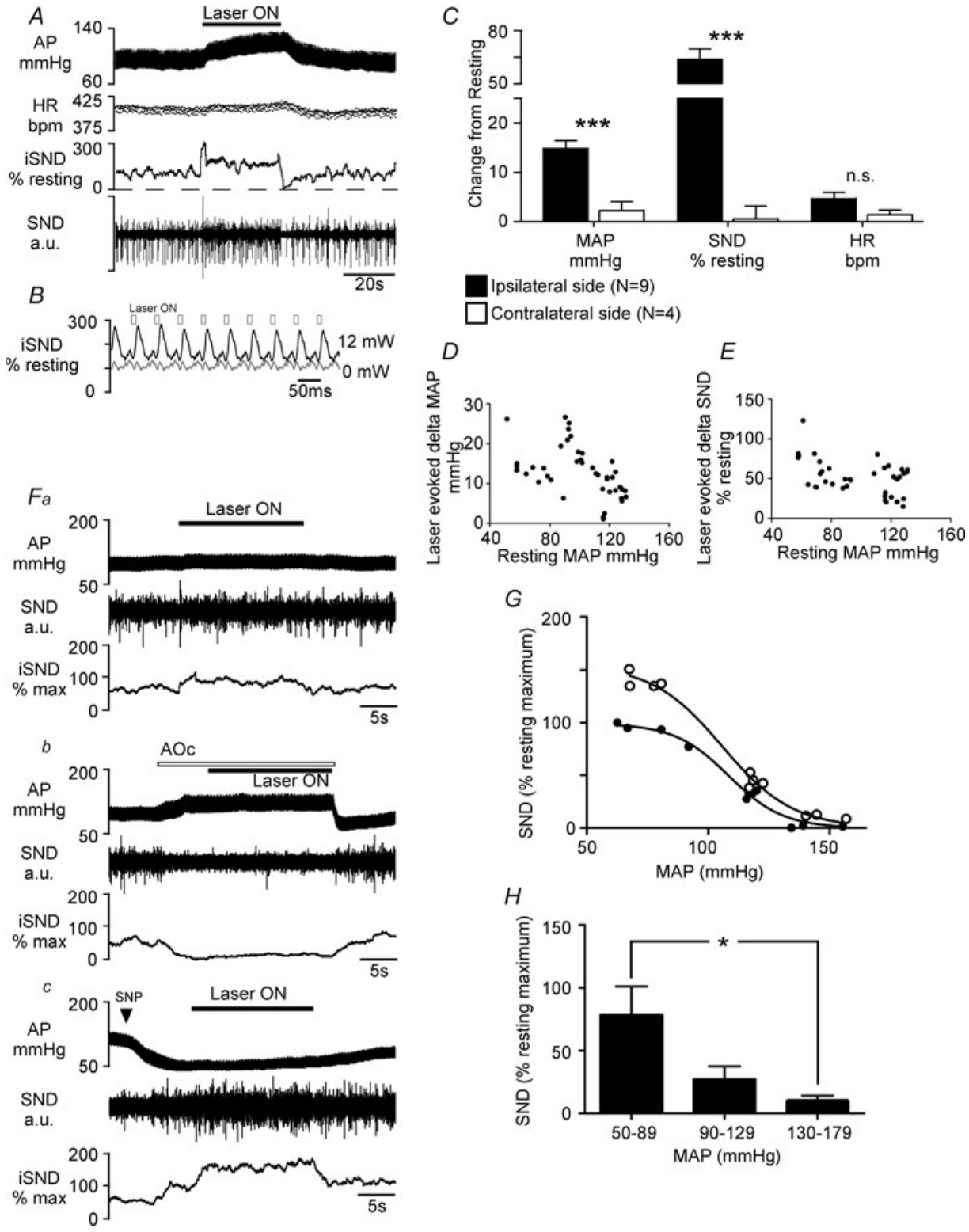

Figure 3. Photostimulation of ChR2-expressing RVLM neurons activates BP. HR and SND
A, representative examples of the cardiovascular effects produced by photostimulation of the RVLM with pulsed laser light (20 Hz, 10 ms, 9 mW). Traces from top to bottom represent arterial pressure (AP), heart rate (HR), integrated sympathetic nerve discharge (SND; rectified and integrated with 2 s time constant and expressed relative to resting discharge, 0% representing the value observed at saturation of the baroreflex and 100% the resting level), and raw SND. *B*, a waveform average of rectified SND triggered by laser pulse onset. This excerpt is from the animal shown in *A*. *C*, group data showing the effect of photostimulation (30 s trains, 20 Hz,

from the vertical (Fig. 4*A*). The sample (59 neurons in 11 rats) included 35 neurons that were silenced by raising BP in the range of 130–160 mmHg via gradual aortic occlusion (cardiovascular neurons; Fig. 4*Ba* and *b* and *E*), 17 neurons that were insensitive to acute increases in arterial pressure up to 160 mmHg and to increases in end-tidal CO_2 up to 8% (tonic neurons; Fig. 4*G*) and eight respiratory neurons classified as expiratory ($n = 6$) or inspiratory ($n = 2$) based on the timing of their burst of action potentials relative to the phrenic nerve discharge. In two rats, we tested whether the photoactivated cardiovascular neurons had a spinal axon. In six cases out of a sample of 11 cells, thoracic spinal cord stimulation produced constant latency spikes indicative of antidromic activation (mean antidromic latency: 42 ± 9.9 ms; range 9.9–79 ms). Most neurons (5/6; e.g. Fig. 4*A* and *C*) had slowly conducting axons (latency between 30 and 79 ms; axonal conduction velocity estimate between 0.44 and 1.2 m s^{-1}) which is a diagnostic feature of the cardiovascular neurons that belong to the C1 cell group (Schreihofer & Guyenet, 1997). The other neuron had a shorter antidromic latency (9.9 ms; conduction velocity estimate: 3.5 m s^{-1}), which has been associated previously both with a subset of C1 neurons and with cardiovascular neurons that lack the catecholaminergic phenotype (Schreihofer & Guyenet, 1997).

A large majority of the cardiovascular neurons (26/34, 77%) were vigorously activated by the light pulses (Fig. 4*Ba* and *b*). These neurons had a moderate level of activity at rest and were typically silenced by increasing BP in the 130–150 mmHg range (Figs 4*Ba* and *b* and 5*A*). Photostimulation (20 Hz, 10 ms) more than doubled their resting activity (from a resting level of 11.8 ± 1.9 to 24.1 ± 1.5 Hz, $P < 0.0001$; Figs 4*Ba* and *b* and 5*B*). In these neurons each light pulse typically induced a single action potential (Fig. 4*Da*) or, more rarely, two (Fig. 4*Db*). Figure 4*Da* shows a peri-event triggered histogram of a neuron that fired a single action potential every light pulse with perfect fidelity and invariant latency (jitter < 1 ms). In addition, photostimulation suppressed the occurrence of most action potentials between light pulses (Fig. 4*Da* and *b*). As a result, the action potentials of these neurons became strictly synchronized to the light pulses and their discharge rate settled at or very close to the photostimulus frequency (20 Hz; Figs 4*Ba* and *b* and 5*C*). The probability of an action potential occurring during a light pulse was zero within the first 2 ms of the light pulse, around 50% 5 ms after light onset and essentially 100% by the end of the light pulse (Fig. 5*D*). At the end of the photostimulation period, the neurons briefly settled to a level of activity that was lower than the pre-stimulation baseline (Fig. 4*Ba* and *b*). This undershoot, reminiscent of that observed under similar circumstances in the sympathetic nerve discharge (Fig. 3*A*), persisted until BP settled back to the pre-stimulus level and was presumably caused by an increase in baroreceptor feedback.

The rest of the cardiovascular neurons ($n = 8$, 23%) were inhibited during the period of photostimulation (from 21.2 ± 2.2 to 9.9 ± 2.5 Hz, $P = 0.001$; Figs 4*E* and 5*B*). These neurons tended to have a higher resting discharge than the rest of the cardiovascular neurons but the difference was not statistically significant (Fig. 5*A*). They were highly sensitive to increases in BP (from 21.2 ± 2.2 to 1.4 ± 0.8 Hz, $P < 0.001$; Fig. 5*A*). Their inhibition during photostimulation could have largely resulted from an increase in baroreceptor feedback consecutive to the rise in BP because the discharge of the majority of these cells ($n = 6$) had no discernable relationship to the light pulses. However, the rest (3 cells) had a discharge probability that was above average towards the end of the light pulses. This entrainment could conceivably have been caused by a very mild direct photostimulation or it might denote a delayed synaptic inhibition (Fig. 4*F*).

The tonic and baroinsensitive neurons ($n = 17$) were unaffected by the laser light (from 10.5 ± 2.0 to 10.5 ± 2.0 Hz, $P = 0.81$; Figs 4*G* and 5*B*). Also, their probability of firing was the same during and between the light pulses (Figs 4*H*, 5*C*).

Most of the respiratory cells sampled (7/8) were activated by the trains of laser light. On average, photostimulation increased the activity of these neurons substantially (from 12.4 ± 2.2 to 24.2 ± 3.8 Hz, $P < 0.001$; Fig. 5*B*). However, event-triggered averaging of the type shown in Figs 4*Da* and *b* and 5*C* did not reveal any correlation between their discharge probability and the light pulses.

10 ms pulses, 9 mW) on the ipsilateral ($n = 10$) and contralateral ($n = 4$) side to ChR2 transfection. $^*P < 0.05$, $^{**}P < 0.01$, $^{***}P < 0.001$. *D*, relationship between the increase in BP caused by photostimulation and the resting level of BP (4 data points per rat; 10 rats). *E*, relationship between the increase in SND caused by photostimulation and the resting level of BP (4 data points per rat; 10 rats). *Fa–c*, representative examples of the SND effect produced by photostimulation (20 Hz, 10 ms, 9 mW) at normal (*a*), raised (*b*) or lowered (*c*) AP. Gradual aortic occlusion (AOc) was used to raise AP and sodium nitroprusside (SNP) was used to lower AP. *G*, a representative case demonstrating the effects of photostimulation on SND over a wide range of arterial pressure. SND is expressed relative to the maximum discharge observed when the baroreflex was unloaded with SNP as 100% and the value observed at saturation of the baroreflex representing 0%. *H*, grouped data from *G* ($n = 5$) grouped into tertiles according to arterial pressure. $^*P < 0.05$, multiple comparisons.

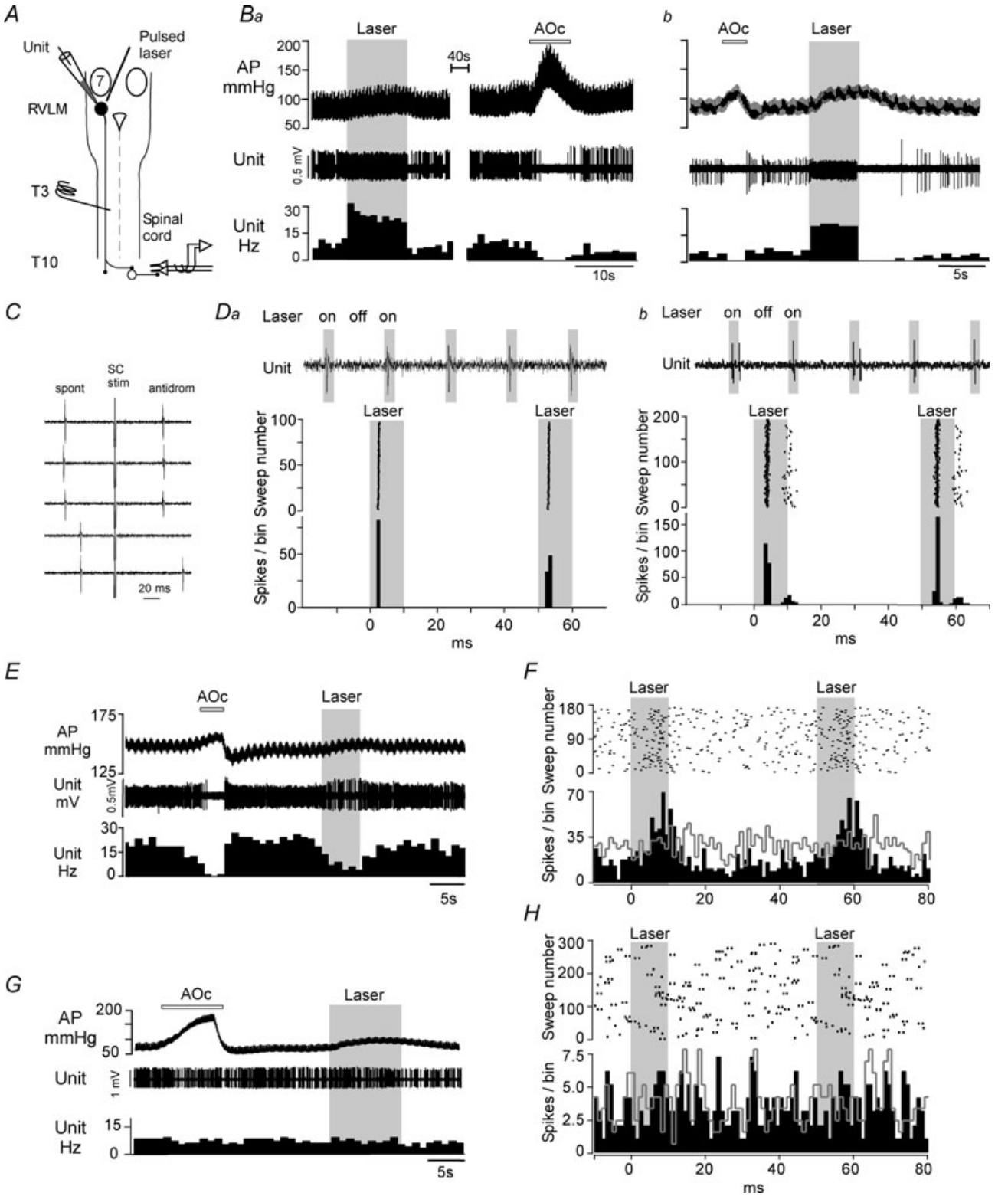

Figure 4. Photoactivation of RVLM cardiovascular neurons
A, experimental design. The fibre optic was inserted at a 20 deg angle from the vertical and single units were recorded using a vertically inserted glass pipette. Antidromic activation was tested by electrical stimulation of the spinal cord at the level of the third thoracic segment. *Ba* and *b*, representative examples of the activation of a single cardiovascular neuron by photostimulation of the RVLM with pulsed laser light (20 Hz, 10 ms, 9 mW). The complete inhibition of the cell activity by a relatively modest increase in BP (AOc, aortic occlusion) is a defining

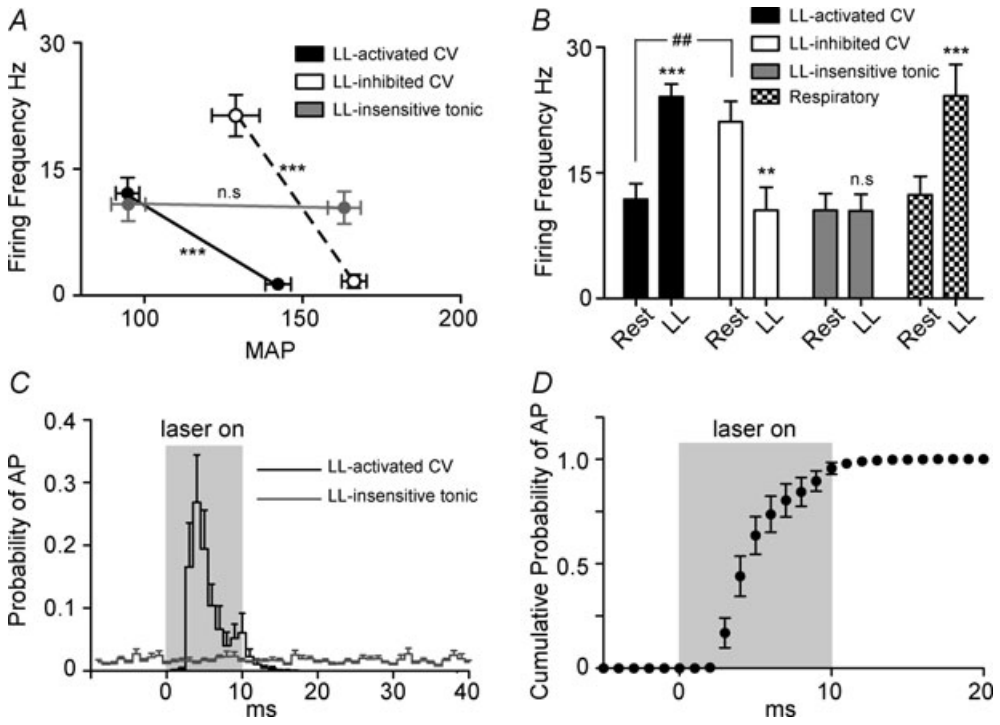

Figure 5. The effects of photostimulation on neurons in the RVLM
A, the effect of raising arterial pressure on the activity of recorded cells. Cells were grouped based on their sensitivity to laser light (LL) stimulation. Both LL activated ($n = 26$) and inhibited cells ($n = 8$) were virtually silenced by raising AP, but LL-insensitive cells ($n = 17$) were unaffected by elevated AP. $^{*}P < 0.05$, $^{**}P < 0.01$. *B*, the effect of photostimulation on the activity of recorded cells. $^{*}P < 0.05$, $^{**}P < 0.01$, $^{***}P < 0.001$ *vs*. resting frequency using paired *t* test. $\#\#P < 0.01$ as indicated using unpaired *t* test. *C*, grouped data from event-triggered histograms (1 ms bin) from LL activated neurons demonstrating that during 20 Hz laser stimulation, virtually all action potentials occur within 10 ms of the laser pulse onset with a large peak occurring 5 ms after the onset of the laser pulse. A subsidiary peak occurred between 9 and 10 ms representing cases when cells fired in couplets. For comparison, the same averaging of LL-insensitive cells shows no relationship with the timing of the laser pulse. *D*, the cumulative probability of the first evoked action potential in LL activated cells during photostimulation. This shows that virtually all laser-evoked action potentials occurred within 10 ms of the laser pulse onset. Cases in which laser pulses failed to evoke an action potential were ignored.

ChR2-expressing neurons are both activated and entrained by the light pulses

In theory, photostimulation of a brain area that contains ChR2-transfected neurons could change the activity of the underlying neurons in several ways. The light should directly activate some neurons because they express ChR2 and photostimulation produces a sufficiently large inward current to trigger action potentials. However, some of these neurons may in turn drive or inhibit ChR2-negative (non-transfected) neurons via mono- or even poly-synaptic connections. Prior work by us and

characteristic of this cell group. Note that the firing rate of both neurons rapidly settled to the frequency of the laser (20 Hz). *C*, collision test performed on one of the cardiovascular neurons demonstrating that this cardiovascular cell had an axonal projection to the spinal cord. The slow antidromic latency (55 ms) identified this cell as a C1 neuron. *Da* and *b*, upper trace: photoactivation of two cardiovascular neurons shown at high time resolution. The response shown in *Da* was the most typical. Each light pulse produced a single action potential at an invariant latency. Lower trace: raster plot and the event-triggered histogram (trigger at onset of light pulse; 1 ms bin) of a period of photostimulation (20 Hz, 10 ms). The cell shown in *Db* occasionally fired a second action potential at the end of the light pulse. This response was uncommon. Note that in both cases, photostimulation suppressed action potentials between light pulses. *E*, example of cardiovascular neuron that was inhibited during photostimulation of the RVLM. This inhibition may have been caused by the rise in BP. *F*, as in *D*, except for the inhibited cell shown in *E*. There is a slight activation of the cell during the laser pulse followed by reduced activity based on the resting activity (shown in grey). This pattern of activity was observed in 3 of 8 cells inhibited by photostimulation. *G*, example of a cell that was sensitive to neither increased AP nor photostimulation. *H*, a raster plot and event triggered histogram for the cell shown in *G*.

others indicates that neurons that are both strongly activated and faithfully entrained by the light pulses are very likely to express ChR2 and be directly activated by the light pulses. The first objective of the experiments described next was to ascertain that the cardiovascular neurons conform to this assumption. Secondly, we also wished to test the converse proposition, namely that the RVLM neurons whose discharge bore no relationship with the light pulses were ChR2-negative, regardless of whether their mean level of activity was enhanced by the stimulus.

To address this question, we labelled 12 neurons with biotinamide using the juxtacellular method (6 rats). The sample included seven strongly entrained and activated cardiovascular neurons that were all mCherry-positive (Fig. 6*Aa* and *b*). The sample also included five neurons whose discharge displayed no correlation with the light pulses when examined by peri-event histograms. None of these five neurons had a detectable level of mCherry (Fig. 6*Ba* and *b*). Four of these mCherry negative neurons, including that illustrated in Fig. 6*Ba* and *b*, were respiratory phasic, three having an expiratory decrementing (E2) pattern and the one, an inspiratory-synchronous discharge (I-all). These four mCherry negative neurons were strongly activated by photostimulation. The remaining mCherry negative neuron was baro-insensitive and discharged tonically at rest. Photostimulation did not modify its discharge rate nor synchronize its action potentials to the light pulses.

SND evoked by single or twin pulses of laser light applied to the RVLM

Single 10 ms light pulses were applied to the RVLM at a frequency between 0.2 and 0.5 Hz using the standard power setting to determine the latency of the evoked sympathetic response. These light pulses evoked very large bursts of SND (Fig. 7*A*) that were completely suppressed by elevating BP with an intravenous injection of PE (Fig. 7*B*) and were therefore due to the activation of barosensitive, hence presumably vasoconstrictor, sympathetic efferents. Peri-event triggered histograms of SND ($n = 10$ rats) revealed that the evoked burst usually consisted of a single peak with an onset latency of 29 ± 1.0 ms, a latency to peak of 58 ± 2.0 ms and a peak amplitude reaching $1646 \pm 170\%$ of baseline (Fig. 7*C*). In three of the 10 rats (inserts in Fig. 7*C*) a second and much smaller peak was detectable as is

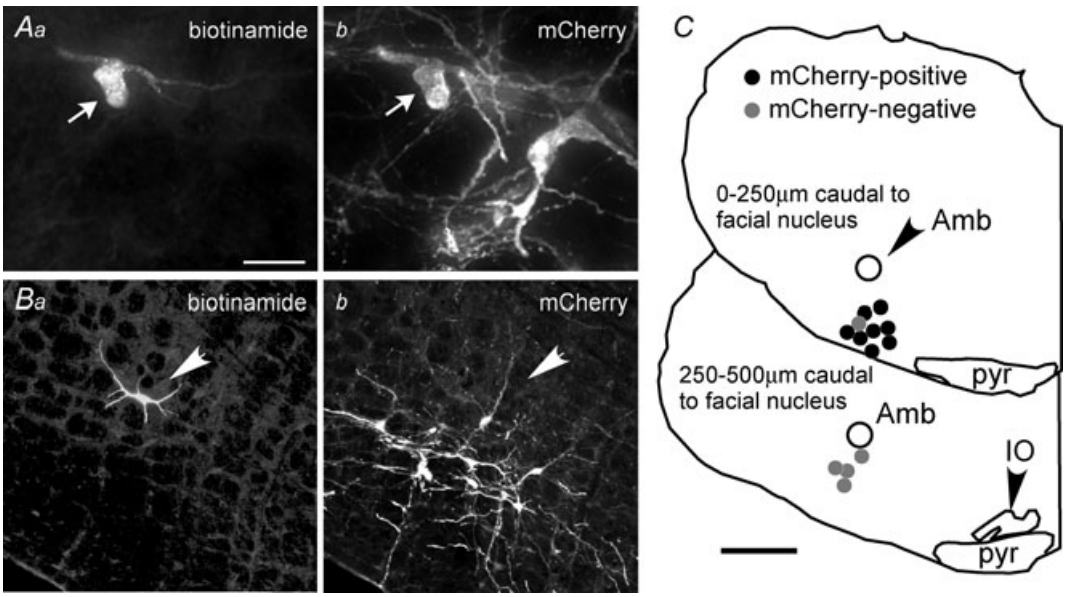

Figure 6. ChR2-expression by RVLM neurons with activity synchronized with light pulses
A, cardiovascular neuron with action potentials synchronized 1 : 1 by the light pulses. This neuron was labelled juxtacellularly with biotinamide following its characterization as barosensitive and photoactivated. It is identified by the presence of green fluorescing Alexa 488 (panel *Aa*). Panel *Ab* shows that the same neuron (arrow) is immunoreactive for the ChR2-mCherry fusion protein (reporter: red fluorescing Cy3). *B*, respiratory neuron (post-inspiratory). This neuron was activated by light trains but its action potentials were not synchronized to the light pulses (*a*: biotinamide; *b*: ChR2-mCherry). This neuron contained no ChR2-mCherry and was located just dorsal to the cluster of neurons that expressed the transgene, i.e. in the Bötzinger region of the RVLM. Scale bar shown in *Aa* represents 25 μm in *Aa* and *b* and 100 μm in *Ba* and *b*. *C*, computer-assisted plots showing the location of the juxtacellularly labelled neurons. The mCherry-positive cardiovascular neurons are in black and the neurons that did not contain detectable levels of the transgene are in grey. Abbreviations: Amb, compact portion of the nucleus ambiguus. IO, inferior olive; pyr, pyramidal tract. Scale bar 0.5 mm.

commonly seen with electrical stimulation of the RVLM region (Morrison *et al.* 1988).

A profound and long-lasting reduction in sympathetic nerve activity ($-87.3 \pm 4.3\%$ from baseline) followed the peak evoked by the light pulse (Fig. 7*C*). This inhibition was maximal 264 ± 15 ms after light onset and SND returned to pre-stimulus levels 1.3 ± 0.16 s after the onset of the light pulse. A classic paired pulse protocol was used to examine the impact of this period of post-stimulus depression on the magnitude of a second evoked response elicited at various intervals after the first. A representative case (Fig. 7*D*) and the group data (Fig. 7*E*) illustrate the powerful occlusion of the second evoked response and the long duration of the paired pulse inhibition. The second evoked response was inhibited by a maximum of $77 \pm 3.7\%$ when the light pulse was delivered within 300 ms of the first one. Half recovery required an interval of between 600 and 1000 ms between light pulses, although significant inhibition often remained up to 2 s after the initial pulse ($F_{6,41} = 29.9$, $P < 0.001$).

Discussion

The new findings of this study are as follows. We provide additional evidence for the specificity of the PRSx8-ChR2 lentivirus by showing that GABAergic and glycinergic neurons did not express the transgene. Lentiviral-mediated expression of ChR2 by the C1 cells enables precise temporal control of the action potentials

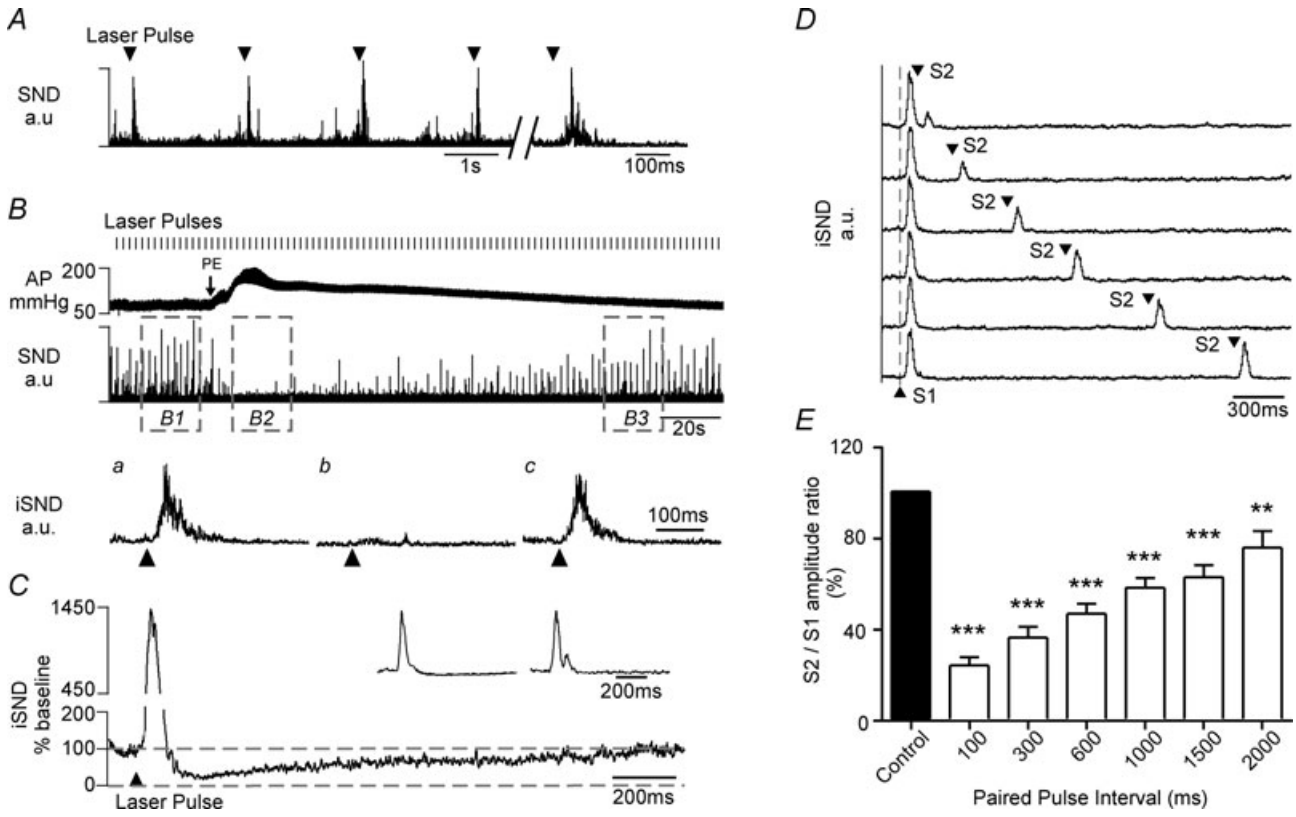

Figure 7. The effects of low frequency photostimulation on SND
A, a representative recording demonstrating the effects of a single 20 ms pulse of laser light on rectified SND. Laser pulses evoked large, reproducible burst in SND, followed by a reduction in spontaneous SND between the laser-evoked bursts. The far right of the trace shows an expanded trace of the same stimulus. *B*, laser-evoked SND bursts are barosensitive. The upper trace represents a recording where phenylephrine (PE) was infused I.V. while 10 ms pulses were delivered at continuously 0.5 Hz. The SND burst is clearly abolished when AP is raised above 150 mmHg. *Ba–c*, laser pulse triggered waveform averages of SND bursts at three time points in *B*, demonstrating the attenuation of the burst by raised AP (*b*) and the recovery of the burst when AP returns to normal levels (*c*). *C*, a laser pulse triggered waveform average of a representative case. This case shows that after the initial burst, SND falls below baseline before slowly returning to pre-stimulus levels. Inset: two other cases where a small second peak was present. *D*, a representative example of the results from the paired-pulse paradigm, where a second pulse is delivered at a set latency after the initial pulse. This uncovered a post-stimulus inhibition of the paired pulse that recovered as the paired pulse latency increased. *E*, grouped data ($n = 6$) for *D*. $^{*}P < 0.05$, $^{**}P < 0.01$, $^{***}P < 0.001$ *vs.* control.

of these neurons by light pulses. Photostimulation of ChR2-transfected RVLM neurons activates vasomotor SND and raises arterial pressure consistent with the postulated role of the C1 neurons in circulatory control. We provide evidence that the RVLM neurons that are directly photoactivated by ChR2-induced inward current can be distinguished from non-transfected neurons whose activation is network driven because only the former have action potentials that are strictly synchronized with the light pulses.

Selectivity of ChR2 expression after administration of PRSx8 lentivirus

In general the selectivity of transgene expression by viral vectors depends on a combination of three factors: promoter selectivity, viral tropism and titre (Nathanson *et al.* 2009). The first two are highly dependent on the brain region, i.e. on the individual characteristics of the targeted population (Nathanson *et al.* 2009). In order to obtain consistently high levels of ChR2 expression we used the highest viral titre that we could achieve and we judged the selectivity of the transfection empirically by performing a thorough phenotypic analysis of the transfected neurons. As in our previous study performed with a different batch of the same viral vector (Abbott *et al.* 2009), all visibly mCherry-positive cells were neurons and these neurons were confined to a relatively small brain region surrounding the injection site. The absence of retrograde transfection is expected from the properties of the VSV glycoprotein (Mazarakis *et al.* 2001). Although the virus injections were placed on average 400 μm more caudal than in our previous study (Abbott *et al.* 2009), we still found that the vast majority (~89%) of the ChR2-expressing neurons contained the transcription factor Phox2b, an endogenous activator of the PRSx8 promoter (Pattyn *et al.* 1999). PRSx8 is usually described as a catecholaminergic neuron-selective promoter (Hwang *et al.* 2001; Lonergan *et al.* 2005; Card *et al.* 2006; Duale *et al.* 2007) although our results suggest that catecholamine neuron-preferring might be a more appropriate descriptor. In the present experiments, the majority of the transfected neurons were indeed C1 cells but high levels of transgene expression were also present in subsets of non-catecholaminergic neurons as observed previously (Abbott *et al.* 2009). A larger percentage of ChR2-expressing neurons were catecholaminergic in the present study than in our prior one (54 *vs.* 33%) because we deliberately targeted a slightly more caudal region of the VLM in which fewer Phox2-expressing neurons are non-catecholaminergic (Stornetta *et al.* 2006). These non-catecholaminergic cells included retrotrapezoid nucleus (RTN) neurons, which we confirmed in the present study by showing that high levels of the transgene were present in very superficial RVLM neurons that contained pre-pro-galanin mRNA (Stornetta *et al.* 2009). GABAergic neurons, though plentiful in the RVLM (Ellenberger, 1999; Stornetta & Guyenet, 1999; Liu *et al.* 2002; Schreihofer & Guyenet, 2003), very rarely expressed detectable levels of the transgene and no glycinergic neurons were labelled. This new information complements the results of our previous study using the same virus (Abbott *et al.* 2009) and is consistent with the fact that, in this region of the brain, Phox2b seems to be almost exclusively expressed by glutamatergic neurons (VGLUT2 mRNA-positive) (Stornetta *et al.* 2006). Overall, these results suggest that the presence of Phox2b is an important factor for the selectivity of transgene expression, but we cannot exclude that a viral tropism favouring excitatory neurons could also have contributed to the selectivity of the transfection (Nathanson *et al.* 2009). This selectivity was not perfect because 11% of the neurons that contained an observable level of ChR2-mCherry were Phox2b-negative. These undefined cells were generally close to the original injection sites. Conceivably these cells may have been damaged and their lack of Phox2b immunoreactivity could have been a problem of histological detection.

The electrophysiological evidence also suggests that a high level of transgene expression was limited to Phox2b-expressing neurons and did not occur in inhibitory neurons. RTN neurons and cardiovascular neurons, which are predominantly Phox2b-expressing C1 neurons, are the only neurons that we have been able to entrain to the laser pulses on a one-to-one basis (Abbott *et al.* 2009; present study). Such entrainment requires that the light pulses produce sufficient depolarizing current to trigger an action potential reliably and therefore presumably requires a high level of ChR2 expression. The respiratory neurons of the Bötzinger region which are inhibitory (GABA- and/or glycinergic) (Ellenberger, 1999; Tanaka *et al.* 2003) could not be entrained in such a fashion, consistent with the notion that they expressed no or insufficient levels of the transgene to be directly photo-activatable.

In summary, the present results indicate that the PRSx8 promoter caused the expression of high levels of transgene primarily in Phox2b-positive neurons. Some low-level non-selective expression also occurred, especially in the immediate vicinity of the injection sites. We found no evidence that this non-selective expression was sufficiently high to enable neurons to respond directly to light but this possibility cannot be categorically eliminated. Over half of the ChR2-positive neurons were C1 cells. These cells also typically expressed a high level of transgene, consistent with the fact that a frank majority of the barosensitive neurons recorded at the rostral end of the cell group were entrained on a pulse by pulse basis by the light.

Photoactivation of the vasomotor neurons

On average, 77% of the barosensitive neurons sampled within the very rostral part of the RVLM were robustly photoactivated. Based on prior evidence, up to 91% of these barosensitive neurons are bulbospinal and hence presumably 'presympathetic' (Schreihofer & Guyenet, 1997) and, based on intracellular or juxtacellular labelling, 26 to 75% of them are C1 neurons (Lipski *et al.* 1995; Schreihofer & Guyenet, 1997). The high level of transgene expression observed by histology within the region where recordings were obtained (70% of C1 cells labelled) is consistent with the photosensitivity of the recorded barosensitive units. The activation of the barosensitive cells was phase-locked to the light pulses and most often occurred with constant latency after the onset of the light pulses. Such precise entrainment is the typical response of ChR2-transfected neurons to pulsed laser light (Boyden *et al.* 2005; Gradinaru *et al.* 2007; Adamantidis *et al.* 2007). By labelling the recorded neurons with biotinamide we were able to demonstrate that neurons with action potentials that were phase-locked to the light pulses were ChR2-transfected. Neurons devoid of detectable ChR2-mCherry did not exhibit phase-locked firing even when their mean discharge rate was substantially elevated by photostimulation of the RVLM. This was the case of the phasically active respiratory neurons that we encountered. This observation can probably be explained by the fact that these respiratory neurons are downstream from RTN neurons that also expressed ChR2 (Abbott *et al.* 2009).

Pulsed laser light produces no cardiorespiratory effect following transfection of RVLM neurons with a PRSx8-containing lentivirus that expresses a photo-insensitive transgene (Abbott *et al.* 2009). Additional evidence of the specificity of the photo stimulus was provided in the present study. For instance, the non-barosensitive, non-respiratory neurons of the RVLM (tonic cells) were uniformly insensitive to light.

At least one-quarter of the barosensitive neurons of the RVLM do not express detectable levels of TH (Lipski *et al.* 1995; Schreihofer & Guyenet, 1997). These particular cells probably do not express Phox2b because, in a prior study, we were not able to detect this protein in any TH-negative bulbospinal neuron (Kang *et al.* 2007). Accordingly, we presume that the TH-negative barosensitive neurons are incapable of expressing the transgene at a level high enough to respond to light but we admit lacking direct evidence to support this claim. By electrophysiology, we did find a 25% subset of rostral RVLM cardiovascular neurons that could not be activated by light. Several of these cells could have been of the non-catecholaminergic variety judging from the fact that their resting discharge rate was well above average (Schreihofer & Guyenet, 1997), but these highly active neurons could also have been non-transfected fast-conducting C1 neurons. These barosensitive neurons were in fact inhibited by photostimulation. In some of them, the inhibition seemed commensurate with a simple passive baroreflex effect. In other cases, the inhibition seemed greater than might have been expected from the baroreflex feedback and could denote the existence of synaptic inhibition unrelated to this feedback. PNMT-immunoreactive terminals establish symmetric synapses with both PNMT-negative and PNMT-immunoreactive RVLM neurons (Milner *et al.* 1989). This feature is indicative of a possible recurrent auto- or cross- inhibition between C1 neurons and of some form of feed-forward control of other RVLM neurons by the C1 neurons. Such synaptic connections could conceivably account for two observations made in the present study namely light-induced inhibition of some of the RVLM neurons beyond the level expected from a simple baroreflex feedback and action potential suppression between the light-induced spikes.

In summary, precise temporal control of the action potentials of the barosensitive neurons could be achieved by pulsed laser light. The photosensitive population included many C1 neurons as shown by the histology and by the fact that a majority of the photoactivated cardiovascular neurons identified as bulbospinal had very low axonal conduction velocities (Schreihofer & Guyenet, 1997). We have not excluded the possibility that the non-catecholaminergic fraction of the barosensitive neurons might also have been photoactivated, but this is somewhat unlikely because these neurons probably do not express Phox2b. Finally, phase-locking of the action potentials to the light pulses appears to distinguish ChR2-transfected neurons that are directly light-activated from neurons, such as the respiratory neurons, that are driven by synaptic inputs from the former category.

Photoactivation of ChR2-expressing RVLM neurons activates BP and SND

Photoactivation of ChR2-expressing RVLM neurons increased splanchnic sympathetic efferent activity and BP. This evidence extends our previous work which indicated that the rise in BP elicited by photostimulation of ChR2-transfected RVLM neurons is attenuated by partial lesion of the C1 neurons that innervate the spinal cord (Abbott *et al.* 2009). The larger pressor responses produced in the present study (15 *vs.* 5 mmHg) can be explained by the fact that we targeted the virus to a slightly more caudal region of the RVLM which contains a higher density of barosensitive neurons and fewer RTN neurons.

The most impressive sympathetic responses were elicited by single light pulses delivered at low frequency. These evoked responses were presumably caused by the near-synchronous activation of the cardiovascular

neurons observed in single-unit experiments. These evoked responses had characteristics that were generally similar to those evoked by single pulse electrical stimulation with respect to peak onset, peak latencies and paired-pulse inhibition (Brown & Guyenet, 1984; Morrison *et al.* 1988). A single noteworthy difference was observed, namely photostimulation evoked a single peak with a latency consistent with the previously described short-latency peak produced by electrical stimulation of the RVLM (peak latency 58 ms) (Morrison *et al.* 1988; Schreihofer *et al.* 2000). The second, longer-latency SNA peak evoked by electrical stimulation of the RVLM has been previously attributed to the activation of a slow-conducting subset of bulbospinal C1 neurons (Morrison *et al.* 1988; Huangfu *et al.* 1994). As discussed above we obtained direct electrophysiological evidence that the C1 neurons with slow-conducting spinal axons are among the cells that are entrained on a pulse by pulse basis by photostimulation. Therefore, the absence of this late peak cannot be explained by a lack of activation of the unmyelinated C1 neurons. A more likely explanation is that, under our experimental conditions, the late peak of excitation was occluded by the silent period of the preganglionic neurons to be discussed later (McKenna & Schramm, 1983; Yoshimura *et al.* 1987*b*; Lewis & Coote, 2008) or by the release of inhibitory transmitters by the vasomotor neurons (catecholamines, enkephalin, neuropeptide Y) (Yoshimura *et al.* 1987*b*; Inokuchi *et al.* 1990; Inokuchi *et al.* 1993). The final possibility is that the subset of bulbospinal C1 neurons with unmyelinated axons actually lack the ability to generate fast excitatory responses in sympathetic preganglionic neurons. Although these neurons probably contain VGLUT2 mRNA (Stornetta *et al.* 2002*b*), perhaps they do not release glutamate in the IML or they use glutamate for some form of slow metabotropic transmission. If this is correct, the late peak of SND elicited by stimulating the RVLM electrically might result from the activation of fibres of passage, for example descending axons that originate in the raphe or the hypothalamus (Morrison, 1993; Huangfu *et al.* 1994).

Higher frequency stimulation of ChR2-transfected RVLM neurons increased splanchnic SND at steady state by about 64% while increasing BP by around 15 mmHg. The increase in SND was greatly reduced when RVLM stimulation was tested at artificially elevated levels of BP and was enhanced at low BP, indicating that the pressor effect caused by C1 cell stimulation is strongly counteracted by the baroreflex and that the splanchnic efferents that were being activated presumably have a vasoconstrictor role. The slowly developing rise in BP seen during photostimulation at 20 Hz could be partly due to the slow kinetics of vascular smooth muscle contractions. Other potential explanations include the release of vasopressin or other vasopressor substances caused by the activation of C1 cells with projections to the hypothalamus (Tucker *et al.* 1987).

The average rise in BP elicited by high frequency (20 Hz) photostimulation of the RVLM (15 mmHg) was relatively modest in comparison with the effects produced by electrical or glutamate stimulation of this structure in similar preparations (Goodchild *et al.* 1984; Ross *et al.* 1984). The simplest explanation is that photostimulation activated a relatively small fraction of the bulbospinal vasomotor C1 cells, perhaps no more than a quarter. Although 77% of the barosensitive neurons sampled by unit recording were photoactivated, we only explored the region of the RVLM located in very close proximity to the virus injection site. Our histological analysis revealed that many untransfected C1 neurons were present medial to the sampled region. These rostral C1 cells are very likely to be also presympathetic. Moreover, close to half of all bulbospinal C1 cells reside caudal to Bregma level 12.1 mm (Schreihofer & Guyenet, 2000; Paxinos & Watson, 2005), a region of the VLM where few if any C1 cells expressed ChR2 in the present experiments. At first glance, the average rise in BP elicited by high frequency (20 Hz) photostimulation of the RVLM (15 mmHg on average) may seem abnormally small in regard to the increase in splanchnic nerve discharge (64% on average). However, the baroreflex operates close to its saturating point under chloralose anaesthesia (Schreihofer & Guyenet, 2003), and therefore a 64% increase in splanchnic nerve discharge relative to the resting level is not an especially large response for a preparation in which baroreceptor unloading is capable of increasing SND up to 4-fold depending on the resting BP (Fig. 3*G*). These considerations may explain the apparent discrepancy between the small rise in BP and the high percentage increase in SNA. However, it is also possible that splanchnic efferents were being somewhat selectively activated in our experiments. According to the organotopy theory, subgroups of RVLM presympathetic neurons differentially control splanchnic *vs.* other vasoconstrictor sympathetic efferents (McAllen *et al.* 1995). The C1 neurons may contribute to this differential control although contrary evidence has also surfaced (Jansen *et al.* 1995*a*).

In contrast to the relatively modest sympathoactivation elicited by train stimulation of the RVLM, low frequency photostimulation of ChR2-transfected RVLM neurons produced a very large peak of sympathoactivation (1600% of baseline value on average) the magnitude of which seems to surpass that evoked by electrical stimulation (Morrison *et al.* 1988; Schreihofer *et al.* 2000). Paired-pulse stimulation revealed that this evoked response is severely attenuated when the stimulus is delivered at frequencies in excess of 0.5 Hz, providing a plausible explanation for the relatively modest increase in mean SND achieved using 20 Hz stimulation. Unit recording of the C1 cells

did not reveal any accommodation of their discharge during train stimulation at high frequency, suggesting that the high-pass filtering of the evoked sympathetic response may occur at the spinal cord level, possibly as a result of the intrinsic properties of the preganglionic neurons, specifically their strong after-hyperpolarization (AHP) (Yoshimura *et al.* 1986). This AHP is inhibited by noradrenaline (Yoshimura *et al.* 1987*a*; Huangfu *et al.* 1992; Jansen *et al.* 1995*b*) suggesting that co-activation of the A5 noradrenergic neurons might potentiate the sympathoactivation caused by high frequency stimulation of the C1 cells. The sympathetic preganglionic neurons receive many additional inputs, for example from the non-catecholaminergic portion of the bulbospinal RVLM projection, the hypothalamus or the serotonergic neurons of the raphe (Jansen *et al.* 1995*b*; Kolaj & Renaud, 1998; Madden & Morrison, 2006). Each of these inputs could, in theory, up- or down-regulate the sympathoexcitatory effect of the C1 cells simply by altering the intrinsic properties of the preganglionic neurons. The present findings highlight the need for studies to determine to what extent these pathways bias synaptic throughput in the IML *in vivo*, and whether a corruption of this process could contribute to neurogenic hypertension.

Conclusions

Injections of PRSx8-ChR2-mCherry lentivirus into the RVLM caused ChR2 expression in subsets of Phox2b-positive neurons, predominantly of the C1 variety (54%). The action potentials of the ChR2-transfected C1 cells could be precisely controlled with light pulses with the added benefit of virtually limitless stimulus repetition and absence of artifact. Photostimulation of the RVLM caused a sizable increase in sympathetic vasoconstrictor tone. Given that the C1 neurons were the dominant type of ChR2-transfected neuron, the present results provide the most direct evidence yet that C1 cell activation increases vasomotor tone. However, this evidence still falls short of a proof because other cell types were also labelled with ChR2.

References

Abbott SBG, Stornetta RL, Fortuna MG, Depuy SD, West GH, Harris TE & Guyenet PG (2009). Photostimulation of retrotrapezoid nucleus Phox2b-expressing neurons in vivo produces long-lasting activation of breathing in rats. *J Neurosci* **29**, 5806–5819.

Adamantidis AR, Zhang F, Aravanis AM, Deisseroth K & De Lecea L (2007). Neural substrates of awakening probed with optogenetic control of hypocretin neurons. *Nature* **450**, 420–424.

Barman SM & Gebber GL (1985). Axonal projection patterns of ventrolateral medullospinal sympathoexcitatory neurons. *J Neurophysiol* **53**, 1551–1566.

Boyden ES, Zhang F, Bamberg E, Nagel G & Deisseroth K (2005). Millisecond-timescale, genetically targeted optical control of neural activity. *Nat Neurosci* **8**, 1263–1268.

Brown DL & Guyenet PG (1984). Cardiovascular neurons of brain stem with projections to spinal cord. *Am J Physiol Regul Integr Comp Physiol* **247**, R1009–R1016.

Brown DL & Guyenet PG (1985). Electrophysiological study of cardiovascular neurons in the rostral ventrolateral medulla in rats. *Circ Res* **56**, 359–369.

Card JP, Sved JC, Craig B, Raizada M, Vazquez J & Sved AF (2006). Efferent projections of rat rostroventrolateral medulla C1 catecholamine neurons: Implications for the central control of cardiovascular regulation. *J Comp Neurol* **499**, 840–859.

Dampney RA, Goodchild AK, Robertson LG & Montgomery W (1982). Role of ventrolateral medulla in vasomotor regulation: a correlative anatomical and physiological study. *Brain Res* **249**, 223–235.

Drummond GB (2009). Reporting ethical matters in *The Journal of Physiology*: standards and advice. *J Physiol* **587**, 713–719.

Duale H, Waki H, Howorth P, Kasparov S, Teschemacher AG & Paton JF (2007). Restraining influence of A2 neurons in chronic control of arterial pressure in spontaneously hypertensive rats. *Cardiovasc Res* **76**, 184–193.

Ellenberger HH (1999). Distribution of bulbospinal gamma-aminobutyric acid-synthesizing neurons of the ventral respiratory group of the rat. *J Comp Neurol* **411**, 130–144.

Gebber GL, Zhong S & Barman SM (1995). The functional significance of the 10-Hz sympathetic rhythm: A hypothesis. *Clin Exp Hypertens* **17**, 181–195.

Goodchild AK, Moon EA, Dampney RA & Howe PR (1984). Evidence that adrenaline neurons in the rostral ventrolateral medulla have a vasopressor function. *Neurosci Lett* **45**, 267–272.

Gradinaru V, Thompson KR, Zhang F, Mogri M, Kay K, Schneider MB & Deisseroth K (2007). Targeting and readout strategies for fast optical neural control in vitro and in vivo. *J Neurosci* **27**, 14231–14238.

Guertzenstein PG & Silver A (1974). Fall in blood pressure produced from discrete regions of the ventral surface of the medulla by glycine and lesions. *J Physiol* **242**, 489–503.

Guyenet PG (2006). The sympathetic control of blood pressure. *Nat Rev Neurosci* **7**, 335–346.

Guyenet PG, Mulkey DK, Stornetta RL & Bayliss DA (2005). Regulation of ventral surface chemoreceptors by the central respiratory pattern generator. *J Neurosci* **25**, 8938–8947.

Huangfu D, Hwang LJ, Riley TA & Guyenet PG (1992). Splanchnic nerve response to A5-area stimulation in rats. *Am J Physiol Regul Integr Comp Physiol* **263**, R437–R446.

Huangfu D, Hwang LJ, Riley TA & Guyenet PG (1994). Role of serotonin and catecholamines in sympathetic responses evoked by stimulation of rostral medulla. *Am J Physiol Regul Integr Comp Physiol* **266**, R338–R352.

Hwang DY, Carlezon WA Jr, Isacson O & Kim KS (2001). A high-efficiency synthetic promoter that drives transgene expression selectively in noradrenergic neurons. *Hum Gene Ther* **12**, 1731–1740.

Inokuchi H, Yoshimura M, Polosa C & Nishi S (1990). The effects of 5-hydroxytryptamine on cat sympathetic preganglionic neurons in vitro. *Kurume Med J* **37**, 309–312.

Inokuchi H, Yoshimura M, Polosa C & Nishi S (1993). Tachykinins depress a calcium-dependent potassium conductance in sympathetic preganglionic neurons. *Regul Pept* **46**, 367–369.

Jansen ASP, Nguyen XV, Karpitskiy V, Mettenleiter TC & Loewy AD (1995*a*). Central command neurons of the sympathetic nervous system: basis of the fight-or flight response. *Science* **270**, 644–646.

Jansen ASP, Wessendorf MW & Loewy AD (1995*b*). Transneuronal labelling of CNS neuropeptide and monoamine neurons after pseudorabies virus injections into the stellate ganglion. *Brain Res* **683**, 1–24.

Kang BJ, Chang DA, Mackay DD, West GH, Moreira TS, Takakura AC, Gwilt JM, Guyenet PG & Stornetta RL (2007). Central nervous system distribution of the transcription factor Phox2b in the adult rat. *J Comp Neurol* **503**, 627–641.

Kolaj M & Renaud LP (1998). Vasopressins's depolarizing action on neonatal rat spinal lateral horn neurons may involve multiple conductances. *Adv Exp Med Biol* **449**, 201–210.

Lewis DI & Coote JH (2008). Electrophysiological characteristics of vasomotor preganglionic neurons and related neurons in the thoracic spinal cord of the rat: An intracellular study in vivo. *Neurosci* **152**, 534–546.

Lipski J, Kanjhan R, Kruszewska B & Smith M (1995). Barosensitive neurons in the rostral ventrolateral medulla of the rat *in vivo*: Morphological properties and relationship to C1 adrenergic neurons. *Neurosci* **69**, 601–618.

Liu YY, Wong-Riley MTT, Liu JP, Jia Y, Liu HL, Jiao XY & Ju G (2002). GABAergic and glycinergic synapses onto neurokinin-1 receptor-immunoreactive neurons in the pre-Botzinger complex of rats: light and electron microscopic studies. *Eur J Neurosci* **16**, 1058–1066.

Llewellyn-Smith IJ, Minson JB, Pilowsky PM & Chalmers JP (1991). There are few catecholamine- or neuropeptide Y-containing synapses in the intermediolateral cell column of rat thoracic spinal cord. *Clin Exp Pharm Phys* **18**, 111–115.

Lonergan T, Teschemacher AG, Hwang DY, Kim KS, Pickering AE & Kasparov S (2005). Targeting brain stem centres of cardiovascular control using adenoviral vectors: impact of promoters on transgene expression. *Physiol Genomics* **20**, 165–172.

Madden CJ & Morrison SF (2006). Serotonin potentiates sympathetic responses evoked by spinal NMDA. *J Physiol* **577**, 525–537.

Madden CJ & Sved AF (2003). Cardiovascular regulation after destruction of the C1 cell group of the rostral ventrolateral medulla in rats. *Am J Physiol Heart Circ Physiol* **285**, H2734–H2748.

Mazarakis ND, Azzouz M, Rohll JB, Ellard FM, Wilkes FJ, Olsen AL, Carter EE, Barber RD, Baban DF, Kingsman SM, Kingsman AJ, O'Malley K & Mitrophanous KA (2001). Rabies virus glycoprotein pseudotyping of lentiviral vectors enables retrograde axonal transport and access to the nervous system after peripheral delivery. *Hum Mol Genet* **10**, 2109–2121.

McAllen RM, May CN & Shafton AD (1995). Functional anatomy of sympathetic premotor cell groups in the medulla. *Clin Exp Hypertens* **17**, 209–221.

McKenna KE & Schramm LP (1983). Sympathetic preganglionic neurons in the isolated spinal cord of the neonatal rat. *Brain Res* **269**, 201–210.

Milner TA, Morrison SF, Abate C & Reis DJ (1988). Phenylethanolamine N-methyltransferase-containing terminals synapse directly on sympathetic preganglionic neurons in the rat. *Brain Res* **448**, 205–222.

Milner TA, Pickel VM, Morrison SF & Reis DJ (1989). Adrenergic neurons in the rostral ventrolateral medulla: ultrastructure and synaptic relations with other transmitter-identified neurons. *Prog Brain Res* **81**, 29–47.

Moreira TS, Takakura AC, Colombari E & Guyenet PG (2006). Central chemoreceptors and sympathetic vasomotor outflow. *J Physiol* **577**, 369–386.

Morrison SF (1993). Raphe pallidus excites a unique class of sympathetic preganglionic neurons. *Am J Physiol Regul Integr Comp Physiol* **265**, R82–89.

Morrison SF, Milner TA & Reis DJ (1988). Reticulospinal vasomotor neurons of the rat rostral ventrolateral medulla: relationship to sympathetic nerve activity and the C1 adrenergic cell group. *J Neurosci* **8**, 1286–1301.

Nagel G, Szellas T, Huhn W, Kateriya S, Adeishvili N, Berthold P, Ollig D, Hegemann P & Bamberg E (2003). Channelrhodopsin-2, a directly light-gated cation-selective membrane channel. *Proc Natl Acad Sci U S A* **100**, 13940–13945.

Nathanson JL, Yanagawa Y, Obata K & Callaway EM (2009). Preferential labelling of inhibitory and excitatory cortical neurons by endogenous tropism of adeno-associated virus and lentivirus vectors. *Neurosci* **161**, 441–450.

Pattyn A, Morin X, Cremer H, Goridis C & Brunet JF (1999). The homeobox gene Phox2b is essential for the development of autonomic neural crest derivatives. *Nature* **399**, 366–370.

Paxinos G & Watson C (2005). *The Rat Brain in Stereotaxic Coordinates*. Elsevier Academic Press, San Diego.

Pilowsky PM & Goodchild AK (2002). Baroreceptor reflex pathways and neurotransmitters: 10 years on. *J Hypertens* **20**, 1675–1688.

Reis DJ, Morrison S & Ruggiero DA (1988). The C1 area of the brainstem in tonic and reflex control of blood pressure. State of the art lecture. *Hypertension* **11**, I8–13.

Ross CA, Ruggiero DA, Park DH, Joh TH, Sved AF, Fernandez-Pardal J, Saavedra JM & Reis DJ (1984). Tonic vasomotor control by the rostral ventrolateral medulla: effect of electrical or chemical stimulation of the area containing C1 adrenaline neurons on arterial pressure, heart rate, and plasma catecholamines and vasopressin. *J Neurosci* **4**, 474–494.

Ruggiero DA, Ross CA, Anwar M, Park DH, Joh TH & Reis DJ (1985). Distribution of neurons containing phenylethanolamine N-methyltransferase in medulla and hypothalamus of rat. *J Comp Neurol* **239**, 127–154.

Sastry L, Johnson T, Hobson MJ, Smucker B & Cornetta K (2002). Titering lentiviral vectors: comparison of DNA, RNA and marker expression methods. *Gene Ther* **9**, 1155–1162.

Schreihofer AM & Guyenet PG (1997). Identification of C1 presympathetic neurons in rat rostral ventrolateral medulla by juxtacellular labelling in vivo. *J Comp Neurol* **387**, 524–536.

Schreihofer AM & Guyenet PG (2000). Sympathetic reflexes after depletion of bulbospinal catecholaminergic neurons with anti-DβH-saporin. *Am J Physiol Regul Integr Comp Physiol* **279**, R729–R742.

Schreihofer AM & Guyenet PG (2003). Baroactivated neurons with pulse-modulated activity in the rat caudal ventrolateral medulla express GAD67 mRNA. *J Neurophysiol* **89**, 1265–1277.

Schreihofer AM, Stornetta RL & Guyenet PG (2000). Regulation of sympathetic tone and arterial pressure by rostral ventrolateral medulla after depletion of C1 cells in rat. *J Physiol* **529**, 221–236.

Stornetta RL, Akey PJ & Guyenet PG (1999). Location and electrophysiological characterization of rostral medullary adrenergic neurons that contain neuropeptide Y mRNA in rat. *J Comp Neurol* **415**, 482–500.

Stornetta RL & Guyenet PG (1999). Distribution of glutamic acid decarboxylase mRNA-containing neurons in rat medulla projecting to thoracic spinal cord in relation to monoaminergic brainstem neurons. *J Comp Neurol* **407**, 367–380.

Stornetta RL, Moreira TS, Takakura AC, Kang BJ, Chang DA, West GH, Brunet JF, Mulkey DK, Bayliss DA & Guyenet PG (2006). Expression of Phox2b by brainstem neurons involved in chemosensory integration in the adult rat. *J Neurosci* **26**, 10305–10314.

Stornetta RL, Sevigny CP, Schreihofer AM, Rosin DL & Guyenet PG (2002*a*). Vesicular glutamate transporter DNPI/GLUT2 is expressed by both C1 adrenergic and nonaminergic presympathetic vasomotor neurons of the rat medulla. *J Comp Neurol* **444**, 207–220.

Stornetta RL, Sevigny CP, Schreihofer AM, Rosin DL & Guyenet PG (2002*b*). Vesicular glutamate transporter DNPI/VGLUT2 is expressed by both C1 adrenergic and nonaminergic presympathetic vasomotor neurons of the rat medulla. *J Comp Neurol* **444**, 207–220.

Stornetta RL, Spirovski D, Moreira TS, Takakura AC, West GH, Gwilt JM, Pilowsky PM & Guyenet PG (2009). Galanin is a selective marker of the retrotrapezoid nucleus in rats. *J Comp Neurol* **512**, 373–383.

Tanaka I, Ezure K & Kondo M (2003). Distribution of glycine transporter 2 mRNA-containing neurons in relation to glutamic acid decarboxylase mRNA-containing neurons in rat medulla. *Neurosci Res* **47**, 139–151.

Tucker DC, Saper CB, Ruggiero DA & Reis DJ (1987). Organization of central adrenergic pathways: I. Relationships of ventrolateral medullary projections to the hypothalamus and spinal cord. *J Comp Neurol* **259**, 591–603.

Yoshimura M, Polosa C & Nishi S (1986). Afterhyperpolarization mechanisms in cat sympathetic preganglionic neuron in vitro. *J Neurophys* **55**, 1234–1246.

Yoshimura M, Polosa C & Nishi S (1987*a*). Afterdepolarization mechanism in the in vitro, cesium-loaded, sympathetic preganglionic neuron of the cat. *J Neurophys* **57**, 1325–1337.

Yoshimura M, Polosa C & Nishi S (1987*b*). Noradrenaline-induced afterdepolarization in cat sympathetic preganglionic neurons in vitro. *J Neurophys* **57**, 1314–1324.

Author contributions

S.B.G.A., P.G.G. and R.L.S. contributed to conception and design, analysis and interpretation of data, drafting the article or revising it critically for important intellectual content, and final approval of the version to be published. S.B.G.A. and P.G.G. performed the electrophysiological experiments. R.L.S. and G.H.W. designed and prepared the lentivirus and did the anatomical experiments. C.S.S. titred the lentivirus.

Acknowledgements

This work was supported by the following grant from the National Institutes of Health to P.G.G. (HL28785).